Cabanelas, J. C., Serrano, B., González-Benito, J., Bravo, J., & Baselga, J. (2001). Morphology of Epoxy/ Polyorganosiloxane Reactive Blends. *Macromolecular Rapid Communications*, 22 (9), pp. 694-699.

DOI: 10.1002/1521-3927(20010601)22:9<694::AID-MARC694>3.0.CO;2-8

Morphology of Epoxy/Polyorganosiloxane Reactive Blends

*J. C. Cabanelas, B. Serrano, J. González-Benito, J. Bravo, J. Baselga**

Instituto Tecnológico Alvaro Alonso Barba, Universidad Carlos III de Madrid, Av. Universidad 30, 28911 Leganés, Madrid, Spain - E-mail: jbaselga@ing.uc3m.e.s

Communication: The morphology of the diglycidyl ether of bisphenol-A / poly(3-aminopropylmethylsiloxane)(DGEBA/ PAMS) reactive blends was studied by fluores-cence techniques as a function of the initial composition. Some fluorescence results were compared with those from optical and electron microscopy investigations. Several morphological aspects were studied including the distribu-tion of PAMS in the blend. The microsegregation of PAMS was discussed in terms of diffusion restriction of DGEBA through the PAMS dispersed phase.

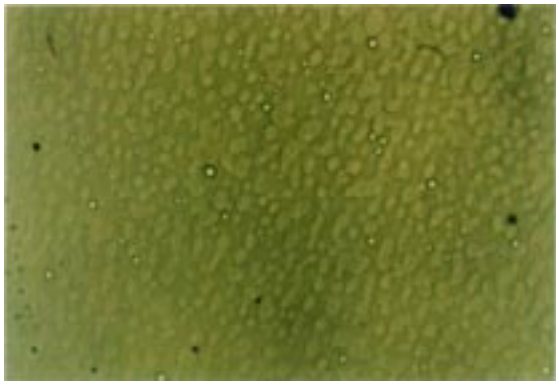

Optical images of samples cured with epoxy/amine in an equivalent ratio of 1.5.

Introduction

Epoxy resins have a number of good mechanical properties, good adhesion and good chemical and thermal resistance for a wide range of different substrates.[1,2] However, these highly crosslinked polymer systems are usually brittle and have limited utility in applications requiring high impact and fracture strength.[3] Thermoplastic[4] or elastomeric materials, such as amino- and carboxy-terminated poly(butadiene-*co*-acrylonitrile) rubbers,[5,6] or the more recently used poly(dimethylsiloxane),[7,8] are added to the reactive system for enhancing the fracture toughness and impact resistance of epoxy networks.

Polysiloxanes have very low glass transition temperatures, T_g, and good thermal stability and elasticity. If employed as epoxy toughening agents they may preserve stable physical properties in the same temperature range as epoxies. Nevertheless, they are immiscible with epoxy resins. To obtain interpenetrated networks and to control the morphology of cured epoxy systems, polysiloxanes bearing reactive end groups (vinyl ether,[9] amino,[7,8,10] epoxy[11] or vinyl[12]) have been used. Reactive blends of these polymers with epoxy resin and amine hardeners are initially homogenous and as the molecular weight increases, the mixture becomes unstable and phase separation occurs.[13] Typically, a fine droplet-like morphology is formed inside the continuous epoxy matrix.

In this work a different approach is proposed. Oligomeric polyorganosiloxanes bearing one primary amino group per monomeric unit are used as curing agents instead of the amine hardener. This system is immiscible at room temperature and as polymerisation proceeds, it becomes partially miscible. The final morphology should be a function, among other factors, of the initial monomer stoichiometry, and this is shown. To the authors knowledge, no previous study on this kind of system has been reported.

Epifluorescence microscopy (EFM) and microfluorescence spectroscopy (MFS) have been successfully employed to characterise phase-separated polymer blends.[14-16] It was demonstrated that fluorescence techniques are sensitive to phase separation at a lower scale than standard techniques such as differential scanning calorimetry (DSC),[17] and that they are not limited by changes in the refractive index of the samples – a disadvantage of optical microscopy.

In this work, both EFM and MFS are employed to study the morphology of siloxane-epoxy thermosetting polymers after an isothermal curing process. Prior to curing, the reactive system is labelled with a well-known sol-

vatochromic probe, dansyl chloride. Three different initial monomer compositions will be studied. As will be demonstrated, although a non-structured thermosetting polymer is to be expected, optical transmission microscopy and MFS show concentration-gradient-dispersed phases ranging between 25 and 100 μm on the cured resin. These results are confirmed by scanning electron microscopy (SEM). The effect of other curing parameters such as temperature or the addition of tensioactives will be reported in a subsequent paper.

Experimental Part

Materials

The diglycidyl ether of bisphenol-A based resin (DGEBA), supplied by Gairesa, had an epoxy equivalent weight of 188 g · (equiv. epoxy)$^{-1}$, as determined by acid titration. The main species consists of 96.5% of pure DGEBA ($\bar{M}_n$ = 340 g · mol^{-1}, $n = 0$); the ratio of secondary hydroxyl groups to epoxy groups was 0.069 ($n = 0.035$), as determined by size exclusion chromatography (SEC) (Shimadzu LC9A).

A highly functionalised polysiloxane curing agent, poly(3-aminopropylmethylsiloxane) (PAMS), was synthesised from 3-aminopropylmethyldiethoxysilane (from ABCR) by monomer hydrolysis and condensation at room temperature, as reported in the literature.[18] The polymer was characterised by SEC, vapour pressure osmometry (VPO; Knauer) and ^{29}Si NMR spectroscopy (Gemini). Number-average molecular weight measured by VPO was 1 620 ± 90 g · mol^{-1} and 1 570 g · mol^{-1} by ^{29}Si NMR, with an amine equivalent of 58.5 g · (equiv. active hydrogen)$^{-1}$.

The synthesised polymer consists of 86% linear (HO-[RSiR'O]$_x$-H) with x = 20, and 14% low molecular weight cyclics fraction (4–5 monomer units). T_g of PAMS is −65 ± 2 °C (DSC, 10 K · min^{-1}).

For fluorescent labelling, a portion of 1,5-dimethylaminonaphthalen-5-sulfonyl chloride (dansyl chloride, DNS; Molecular Probes) chloroform solution was added to PAMS (1 : 5 000 v/v) and heated at 60 °C for 16 h; the final DNS concentration was around 10^{-4} M as determined by UV/VIS spectrophotometry.

Cured Samples

Samples with different epoxy/amine equivalent ratios (r_{EQ}) were prepared by mixing DGEBA and PAMS in a flask with continuous stirring. A drop of the reaction mixture was placed between two glass slides and cured at 60 °C for a sufficient period of time to reach limiting conversion. The thickness of the films was 100 ± 10 μm. The T_gs of the isothermal cured samples was measured by DSC (Perkin Elmer DSC7), on a dynamic scan at 20 K · min^{-1}, under a dry nitrogen atmosphere. Conversion was measured by FT-NIR spectroscopy (Perkin Elmer GX2000), according to the method described in literature.[19,20] Characterisation data are presented in Table 1, which also includes the fluorophore concentration as well as the epoxy conversion (α). The ultimate T_g and the conversion obtained in a direct dynamic curing from 20 °C to 250 °C at 20 K min^{-1} are also presented.

Table 1. T_g (DSC) and epoxy conversion, α (FT-NIR), of cured samples under isothermal (60 °C) and dynamic (20 K · min^{-1}) conditions.

r_{EQ}	Isothermal cure			Dynamic curing		
	t / min	α	T_g / °C	α	$T_{g,max}$ [a] / °C	DNS [b] / mol · kg^{-1}
1.5	90	0.632	46	0.658	59	3.0×10^{-4}
1.0	70	0.792	84	0.852	134	4.0×10^{-4}
0.8	60	0.836	81	0.985	142	4.8×10^{-4}

[a] $T_{g,max}$: the maximum T_g that can be obtained at the highest curing temperature.
[b] Dansyl concentration in the reaction mixture; the concentration in PAMS component is the same in all samples.

Microscopy Measurements

Two different optical microscopes were employed. A Labophot microscope (Nikon) provided with photographic camera was used for transmission optical microscopy (TOM) and epifluorescence microscopy (EFM) imaging observations. Objectives of × 10 and × 40 with numeric apertures of 0.25 and 0.65, respectively, were used. In EFM measurements, a 100-W Hg arc lamp was employed. The excitation beam was filtered with a bandpass filter to transmit in the range 330–380 nm. The sample emission was separated from the excitation beam by a dichroic mirror (excitation wavelength < 400 nm) and a barrier filter (emission wavelength (λ_{em}) < 420 nm).

An Axiovert 100 TV inverted microscope (Carl Zeiss Jena), coupled with a 400-μm optical fibre to an Acton Spectra-Pro-150 monochromator (2 400 lines), was employed for microfluorescence spectroscopy (MFS) measurements. For measuring the fluorescence response distribution along the sample surface, two different experiments were carried out. In the first one (intensity drive), a rectilinear trajectory along the sample was selected in such a way that several fluorescent domains were crossed; sample was excited at 340 nm with an interference filter, and fluorescence, at fixed emission wavelength (460 nm), was measured from spots of size about 6 μm (field diaphragm) at length intervals of 5 μm. In the second experiment (spectra drive), instead of fluorescence intensity, the complete fluorescence spectra were collected. All spectra were corrected using a homemade calibration file.

SEM observations were performed on Au/Pd-coated samples in an XL30 SEM microscope (Phillips). X-ray semiquantitative microanalysis was performed in SEM with an EDAX DX4i detector.

Results and Discussion

Curing of Epoxy Resin

From an inspection of Table 1, the highest epoxy conversion is obtained for r_{EQ} = 0.8 for both the isothermal and dynamic curing schedules. Comparing with r_{EQ} = 1, although different conversions are attained, both samples

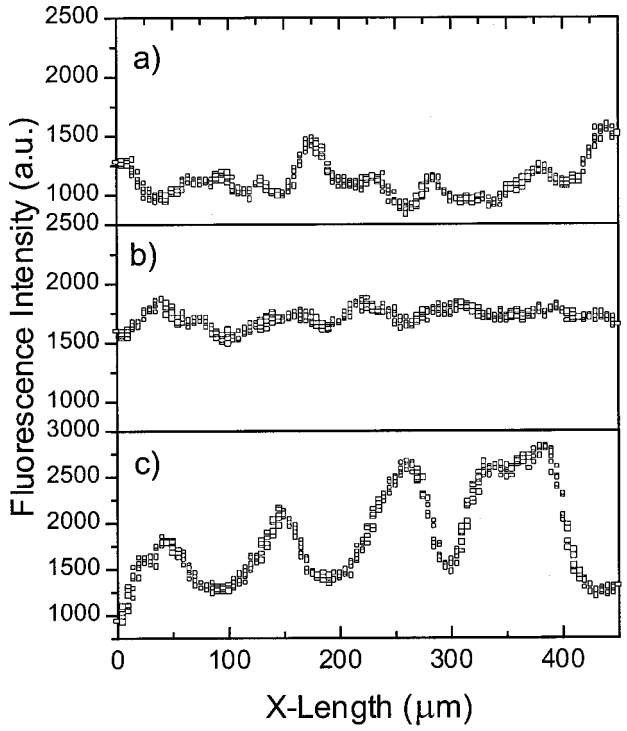

Figure 1. Intensity drive of fluorescence ($_{em}$ = 460 nm) along a random linear trajectory for cured samples with different stoichiometric ratios: (a) r_{EQ} = 1.5; (b) r_{EQ} = 1.0; (c) r_{EQ} = 0.8.

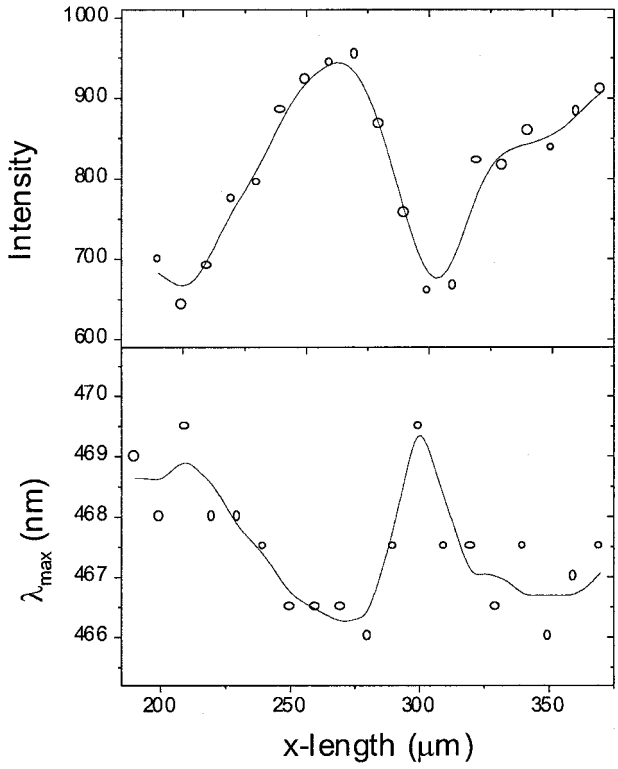

Figure 2. Intensity and wavelength at the maximum of the emission spectra of DNS for a sample with r_{EQ} = 0.8. The *x*-axis has the same interval as that shown in Figure 1c.

present a similar T_g within experimental error. In a dynamic cure, the sample cured at the stoichiometric ratio reaches only 85% epoxy conversion and its maximum T_g is lower than that obtained with a slight excess of amine component (r_{EQ} = 0.8). For the sample cured with an excess of epoxy (r_{EQ} = 1.5) both the conversion and T_g are the lowest. These results are surprising and suggest that epoxy diffusion is restricted within the polymerisation mass.

Microfluorescence Spectroscopy

Using microfluorescence spectroscopy, the fluorescence intensity over a linear trajectory, at $_{em}$ = 460 nm, was recovered for each sample. In Figure 1 an example of three trajectories is presented. A set of consecutive peaks and valleys are observed reflecting the heterogenous distribution of the fluorescent component with some periodic fluctuation of fluorescence intensity in all samples. Since dansyl is labelled to PAMS, those regions should be rich in PAMS component. The average intensity is roughly proportional to the fluorophore concentration shown in Table 1.

The relative peak-to-valley fluorescence intensity ratio was calculated as the difference between the maximum and minimum intensity referred to the average minimum intensity; results yield values about 1.2, 0.2 and 0.3 for stoichiometries of 0.8, 1 and 1.5, respectively, suggesting that PAMS is more homogenously distributed in the stoichiometric sample. The peak-to-peak distance is about 100 μm for r_{EQ} = 0.8 and decreases to about 75 μm for r_{EQ} = 1 and to about 50 μm for r_{EQ} = 1.5. The size of these fluorescent-dispersed phases decrease as the PAMS content in the sample is decreased.

It is known that DNS fluorescence changes with the polarity and viscosity of its environment.[21,22] At the dispersed phases/matrix interphase the fluorescence intensity decreases (Figure 1) on going from the domain to the matrix; it is therefore necessary to analyse if those changes are a result of variations in fluorophore concentration or in local polarity. Microfluorescence spectra were collected across a representative surface each 10 μm for the sample with r_{EQ} = 0.8. Plots of fluorescence intensity and wavelength at the maximum are presented in Figure 2 as a function of trajectory coordinate. The wavelength at the maximum shifts three nanometers to the blue (from 469 to 466 nm) as we go from the outer side to the inner side of the domain, following a pattern exactly opposite to that of the fluorescence intensity. This very small shift can be attributed to differences in the local polarity because PAMS is the less polar component of the mixture; but since the wavelength shift is very small, and the dansyl emission is very broad, this result confirms that intensity changes come mainly from DNS concentration gradient in the sample, and not from the probe response to the microenvironment. Figure 2 there-

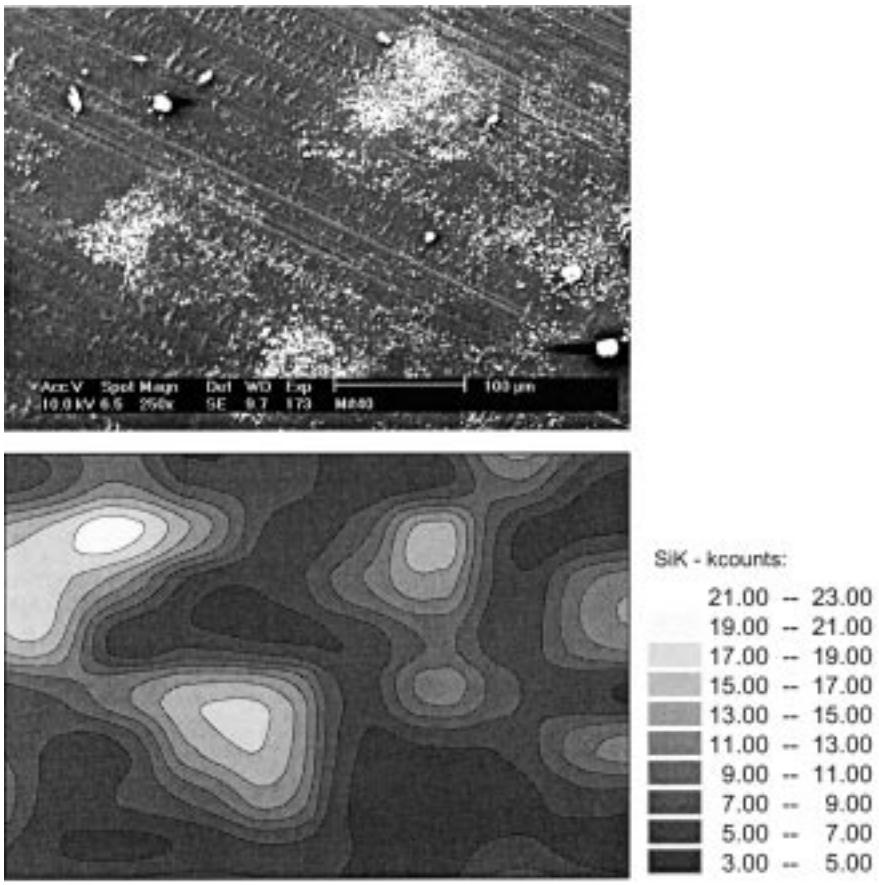

Figure 3. SEM image and contour graph reflecting the distribution of Si atoms on the surface for a stoichiometric sample. The Si concentration is given in kcounts. The clear areas shown in the micrograph (upper) are a result of carbonate formation.

fore leads us to conclude that there is a composition gradient of PAMS inside the fluorescing domains.

To confirm the existence of composition gradients, some SEM observations joined with EDAX quantification of silicon atoms distribution were done on the stoichiometric system, the most homogeneous. A mapping of the Si surface concentration profile was done measuring silicon X-ray K-line intensity in a 500 300 µm region. 15 15 points were examined. Figure 3 shows the SEM image and Si distribution in a grayscale contour map. The polysiloxane component in the thermosetting polymer seems to be structured in concentric layers with a concentration gradient that is in agreement with epifluorescence results. The diameter of these Si-rich areas is about 50 µm, in accordance with the intensity drive results (Figure 1). These observations suggest that polymerisation does not take place in the whole reaction mass but instead in a more or less thick boundary around PAMS-rich places.

TOM and EFM

Optical and epifluorescence images are displayed in Figure 4. TOM micrographs show that all samples are heterogeneous. For non-stoichiometric samples (Figure 4a and 4c), the morphology consists of an irregular dispersed phase inside a continuous matrix. With the help of epifluorescence images it is possible to observe that those regions are richer in PAMS (more fluorescent) than the matrix. Nevertheless, an interconnected co-continuous structure can be observed for the stoichiometric sample (Figure 4b); comparison between TOM and EFM images show that the brilliant thin-walled network observed by TOM corresponds to non-fluorescent DGEBA-rich regions. It is interesting to observe that, contrary to what should be expected from simple thermodynamic mixing arguments, PAMS shows only a slight tendency to form the matrix in which DGEBA could be dispersed, even when it is in excess. Interfacial free energy should play an important role in these systems.

For the system rich in DGEBA (Figure 4a), the observed morphology is probably the result of the formation of small sized droplets of PAMS in the epoxy matrix at the beginning of the reaction. Considering that the ultimate T_g for this system is always below the curing temperature (Table 1), interdiffusion may occur at the PAMS/DGEBA interphase enabling polymerisation to

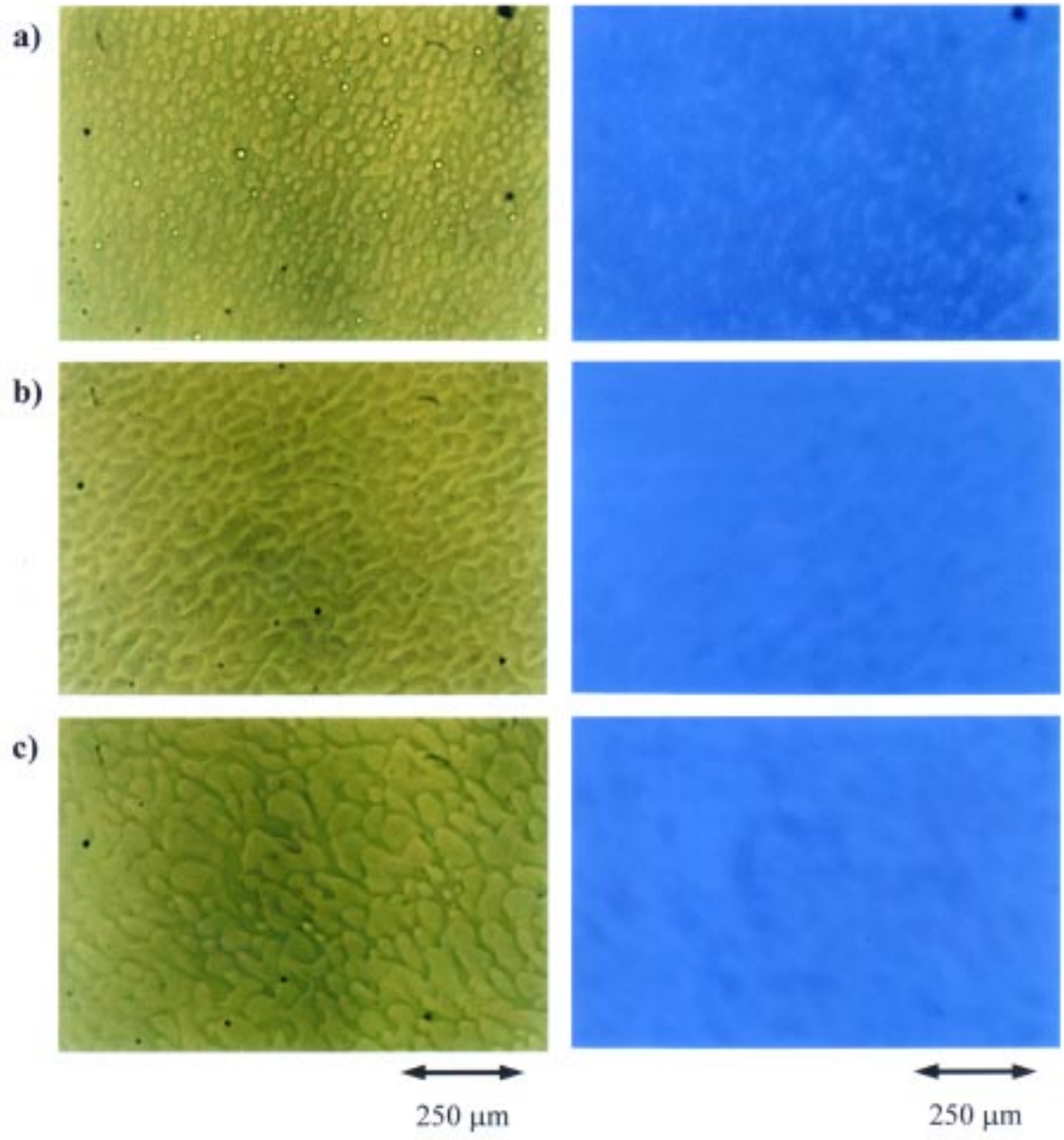

Figure 4. TOM (left) and EFM (right) images of samples cured with different epoxy/amine equivalent ratios: (a) r_{EQ} = 1.5; (b) r_{EQ} = 1.0; (c) r_{EQ} = 0.8. The length of the micrographs corresponds to 1 000 µm.

occur. A highly branched structure may be formed at the interphase inhibiting further diffusion of reactives. As a consequence, the reaction stops at a relatively low conversion (0.63). Epifluorescence micrographs reveal that the consumption of PAMS is not the mechanism by which reaction stops; instead, the restriction of DGEBA diffusion caused by the formation of a gradient network around PAMS particles is most probable.

For the sample with r_{EQ} = 0.8, the same mechanism should operate, but, according to thermal data, higher conversions and T_g are obtained. The only difference between the two non-stoichiometric systems is the size of the PAMS dispersed phases. It seems, therefore, that the size of these PAMS regions may play some role in limiting the conversion that can be achieved. Results suggest that the higher the PAMS phase size, the higher the rate of diffusion of DGEBA through the PAMS dispersed phase, and the less the crosslinked barrier that is formed around them.

Gelation should be excluded, in principle, as the origin of the observed morphology. According to the Flory-Stockmayer theory,[23] the critical conversion should

appear at around $\alpha = 0.19$ for the stoichiometric system, as a result of the high molecular weight of the hardener. For non-stoichiometric systems, the critical conversion should increase, but the results summarised in Table 1 do not show that behaviour.

Conclusions

The morphology of epoxy/poly(3-aminopropylmethylsiloxane) reactive blends has been studied as a function of initial composition. The polysiloxane component was labelled with the dansyl moiety, a well-known solvatochromic fluorescence probe. Fluorescence intensity profiles were recovered from random linear trajectories over the sample surface and average domain sizes were estimated from the valley-to-valley values. It was observed that the size of the PAMS-rich phase increases with PAMS content. It was also observed that PAMS concentration was not uniform along the fluorescent domains. SEM observations confirm the existence of a PAMS gradient around the PAMS dispersed phase and also the low concentration of PAMS in the epoxy-rich phase. We conclude therefore that polymerisation takes place inside the fluorescent PAMS-rich phase. Taking into account values of limiting conversion and thermal data, we conclude that a highly crosslinked barrier around PAMS phase is formed. This barrier restricts diffusion of DGEBA and stops the reaction, at least for the system rich in DGEBA. For the system rich in PAMS, the diffusion restriction seems to be not very important.

Acknowledgement: This research was supported by the *EU*, Brite-EuRam BE97-4472, and by *CAM*, programa de grupos estratégicos, contrato programa 2000–2003. The authors gratefully acknowledge the contribution of Dr. *I. F. Pierola* from *UNED* in the acquisition of the epifluorescence images presented in this work.

[1] C. A. May, "*Epoxy Resins; Chemistry and Technology*", Marcel Dekker, New York 1988.
[2] T. M. Goulding, "Epoxy Resin Adhesives", in: *Handbook of Adhesive Technology*, A. Pizzi, K. L. Mittal, Eds., Marcel Dekker, New York 1994, p. 531.
[3] A. J. Kinloch in: *Rubber-Toughened Plastics*, C. K. Riew, Ed., ACS, Washington 1989, p. 68.
[4] A. Bonnet, J. P. Pascault, H. Sautereau, *Macromolecules* 1999, *32*, 8524.
[5] T. Ohnaga, W. Chen, T. Inoue, *Polymer* 1994, *35*, 3774.
[6] D. Chen, J. P. Pascault, J. P. Sautereau, G. Vigier, *Polym. Int.* 1993, *32*, 369.
[7] Q. J. Wang, O. Kwon, H. Kang, T. C. Ward, J. E. McGrath, *Polym. Prepr.* 1998, *39*, 546.
[8] T. Kasemura, S. Takahashi, K. Nishihara, C. Komatu, *Polymer* 1993, *34*, 3416.
[9] F. Cazaux, X. Coqueret, "*III Conference on Silicones in Coatings*", Barcelona, March 2000, paper 8.
[10] [10a] S. S. Lee, S. C. Kim, *J. Appl. Polym. Sci.* 1997, *64*, 941; [10b] S. S. Lee, S. C. Kim, *J. Appl. Polym. Sci.* 1998, *69*, 1291.
[11] S. Hou, Y. Chung, C. Chan, P. Kuo, *Polymer* 2000, *41*, 3263.
[12] W. He, *J. Appl. Polym. Sci.* 1997, *69*, 619.
[13] C. K. Riew, Ed., "*Rubber-Toughened Plastics*", ACS, Washington 1989.
[14] T. D. Z. Atvars, I. Esteban, B. Illera, B. Serrano, M. R. Vigil, I. F. Piérola, *J. Luminesc.* 1997, *72–74*, 467.
[15] D. Dibbern-Brunelli, T. D. Z. Atvars, *J. Appl. Polym. Sci.* 1995, *55*, 889.
[16] B. Serrano, J. Baselga, J. Bravo, F. Mikes, L. Sesé, I. Esteban, I. F. Piérola, *J. Fluoresc.* 2000, *10*, 2.
[17] H. Morawetz, *Science* 1979, *203*, 405.
[18] R. S. Neale, *Ind. Eng. Chem. Prod. Res. Dev.* 1980, *16*, 639; *Chem. Abstr.* 1980, *93*, 20704j.
[19] V. A. Bershtein, V. M. Egorov, "*Differential Scanning Calorimetry of Polymers*", Ellis Horwood, NewYork 1994.
[20] A. López, P. Prendes, M. Paaos, M. Paz, S. Paz, *Macromolecules* 1998, *31*, 4770.
[21] Y. Li, L. Chan, L. Tyer, R. T. Moody, Ch. M. Himel, D. M. Hercules, *J. Am. Chem. Soc.* 1975, *97*, 3118.
[22] E. Carlier, A. Revillon, A. Guyot, J. Chauvet, *Eur. Polym. J.* 1993, *29*, 819.
[23] [23a] P. J. Flory, "Principles of Polymer Chemistry", Cornell University Press, Ithaca 1969, Ch. IX; [23b] K. Dusek, "*Network Formation Involving Polyfunctional Polymer Chains*", in: *Polymer Networks. Principles of Their Formation, Structure and Properties*, R. F. T. Stepto, Ed., Blackie Academic & Prof., London 1998, Ch. 3, p. 64.